The Stannides $La_3Pd_4Sn_6$, $Ce_3Pd_4Sn_6$, and $Pr_3Pd_4Sn_6$: A New Structure Type with a Complex Three-Dimensional $[Pd_4Sn_6]$ Polyanion

Dirk Niepmann, Rainer Pöttgen,*,† Bernd Künnen, and Gunter Kotzyba

Anorganisch-Chemisches Institut, Universität Münster, Wilhelm-Klemm-Strasse 8, D-48149 Münster, Germany

Bernd D. Mosel*,‡

Institut für Physikalische Chemie, Universität Münster, Schlossplatz 4/7, D-48149 Münster, Germany

Received September 13, 1999. Revised Manuscript Received October 18, 1999

The new stannides $La_3Pd_4Sn_6$, $Ce_3Pd_4Sn_6$, and $Pr_3Pd_4Sn_6$ have been synthesized in quantitative yield by reacting the elements in an arc-melting furnace and subsequent annealing at 970 K. Their structures were determined from single-crystal X-ray data: *Pnma*, $a = 1685.5(2)$ pm, $b = 462.37(9)$ pm, $c = 1562.6(2)$ pm, wR2 = 0.0788, 1561 F^2 values, 80 variables for $La_3Pd_4Sn_6$, $a = 1678.2(3)$ pm, $b = 458.9(1)$ pm, $c = 1556.1(3)$ pm, wR2 = 0.0800, 1539 F^2 values, 81 variables for $Ce_3Pd_4Sn_6$, and $a = 1673.8(4)$ pm, $b = 457.3(1)$ pm, $c = 1554.1(3)$ pm, wR2 = 0.0954, 1529 F^2 values, 81 variables for $Pr_3Pd_4Sn_6$. Striking structural motifs in these structures are distorted $PdSn_5$ square pyramids which are condensed via common tin atoms and via Sn−Sn bonds forming a three-dimensional infinite $[Pd_4Sn_6]$ polyanion that is characterized by strong Pd−Sn (256−285 pm) as well as Sn−Sn (302−336 pm) interactions. Six tin sites occur in the $Ce_3Pd_4Sn_6$ structure. Only the Sn4 atoms have no Sn−Sn contacts. The rare earth atoms fill distorted pentagonal and hexagonal channels within the polyanion. The three crystallographically independent rare earth (RE) atoms have high coordination numbers: 5Ce + 7Pd + 9Sn for Ce1, 4Ce + 6Pd + 9Sn for Ce2, and 5Ce + 7Pd + 9Sn for Ce3. Magnetic susceptibility measurements indicate Pauli paramagnetism for $La_3Pd_4Sn_6$ and Curie−Weiss behavior for $Ce_3Pd_4Sn_6$ (2.51(2) μ_B/Ce) and $Pr_3Pd_4Sn_6$ (3.70(5) μ_B/Pr). No magnetic ordering is detected down to 2 K. $La_3Pd_4Sn_6$, $Ce_3Pd_4Sn_6$, and $Pr_3Pd_4Sn_6$ are metallic conductors with specific resistivities at room temperature of 80 ± 20 $\mu\Omega$ cm ($La_3Pd_4Sn_6$), 65 ± 20 $\mu\Omega$ cm ($Ce_3Pd_4Sn_6$), and 110 ± 20 $\mu\Omega$ cm ($Pr_3Pd_4Sn_6$). The specific resistivity of $Ce_3Pd_4Sn_6$ shows a broad minimum near 16 K, possibly suggesting some Kondo-type interactions. The ^{119}Sn Mössbauer spectrum of $La_3Pd_4Sn_6$ shows two superimposed signals: a singlet at $\delta_2 = 1.88(2)$ mm/s with a line width of $\Gamma_2 = 0.88(2)$ mm/s and a second signal at $\delta_1 = 1.94(2)$ mm/s with a line width of $\Gamma_1 = 0.87(2)$ mm/s, subject to quadrupole splitting of $\Delta E_{Q1} = 1.11(2)$ mm/s. These two signals occur in a ratio of about 5:1 in agreement with the six different tin sites. The cerium and praseodymium stannides show very similar behavior.

Introduction

The location of the 4f level near the Fermi energy in cerium intermetallics can result in a variety of unusual physical properties such as long-range magnetic ordering, Kondo effects, magnetic ordering with anomalously high ordering temperatures, the coexistence of heavy-fermion behavior and superconductivity or valence fluctuation behavior (see refs 1−3, and references therein). The whole bandwidth of such unusual electronic properties has been observed for the various compounds in the ternary systems Ce−Ni−In(Sn) and Ce−Pd−In(Sn) (see refs 4−8, and references therein). Especially the Ce−Pd−Sn system exhibits several ternary stannides: equiatomic CePdSn[9] (TiNiSi type),

† E-mail: pottgen@uni-muenster.de.
‡ E-mail: mosel@uni-muenster.de.

(1) Fujita, T.; Suzuki, T.; Nishigori, S.; Takabatake, T.; Fujii, H.; Sakurai, J. *J. Magn. Magn. Mater.* **1992**, *108*, 35.
(2) Szytuła, A.; Leciejewicz, J. *Handbook of Crystal Structures and Magnetic Properties of Rare Earth Intermetallics*; CRC Press: Boca Raton, 1994.
(3) Nieuwenhuys, G. J. Heavy Fermions and Related Compounds. In *Handbook of Magnetic Materials*; Buschow, K. H. J., Ed.; Elsevier: Amsterdam, 1995; Vol. 9, Chapter 1.
(4) Kasaya, M.; Tani, T.; Iga, F.; Kasuya, T. *J. Magn. Magn. Mater.* **1988**, *76/77*, 278.
(5) Takabatake, T.; Teshima, F.; Fujii, H.; Nishigori, S.; Suzuki, T.; Fujita, R.; Yamaguchi, Y.; Sakurai, J.; Jaccard, D. *Phys. Rev. B* **1990**, *41*, 9607.
(6) Fujii, H.; Inoue, T.; Andoh, Y.; Takabatake, T.; Satch, K.; Maeno, Y.; Fujita, T.; Sakurai, J.; Yamaguchi, Y. *Phys. Rev. B* **1989**, *39*, 6840.
(7) Skolozdra, R. V.; Komarovskaya, L. P. *Izv. Akad. Nauk. SSSR Metally* **1988**, *2*, 214.
(8) Brück, E.; van Sprang, M.; Klaasse, J. C. P.; de Boer, F. R. *J. Appl. Phys.* **1988**, *63*, 3417.
(9) Sakurai, J.; Yamaguchi, Y.; Nishigori, S.; Suzuki, T.; Fujita, T. *J. Magn. Magn. Mater.* **1991**, *90/91*, 422.

10.1021/cm991142z CCC: $19.00
Published on Web 01/04/2000

Table 1. Crystal Data and Structure Refinements for the Orthorhombic Stannides $La_3Pd_4Sn_6$, $Ce_3Pd_4Sn_6$, and $Pr_3Pd_4Sn_6$ (Space Group *Pnma*, No. 62)

empirial formula	$La_3Pd_4Sn_6$	$Ce_3Pd_4Sn_6$	$Pr_3Pd_4Sn_6$
molar mass	1542.18 g/mol	1545.81 g/mol	1560.47 g/mol
lattice constants	$a = 1685.5(2)$ pm	$a = 1678.2(3)$ pm	$a = 1673.8(4)$ pm
(Guinier data)	$b = 462.37(9)$ pm	$b = 458.9(1)$ pm	$b = 457.3(1)$ pm
	$c = 1562.6(2)$ pm	$c = 1556.1(3)$ pm	$c = 1554.1(3)$ pm
	$V = 1.2178(3)$ nm^3	$V = 1.1984(4)$ nm^3	$V = 1.1896(4)$ nm^3
formula units per cell	$Z = 4$	$Z = 4$	$Z = 4$
calculated density	8.48 g/cm^3	8.64 g/cm^3	8.71 g/cm^3
crystal size	$10 \times 20 \times 30$ μm^3	$10 \times 20 \times 40$ μm^3	$10 \times 20 \times 30$ μm^3
transmission (max:min)	1.19	1.36	1.31
absorption coefficient	28.0 mm^{-1}	29.2 mm^{-1}	30.2 mm^{-1}
$F(000)$	2620	2632	2644
θ range	2 to 28°	2 to 28°	2 to 28°
range in hkl	$\pm 21, 0 \le k \le 6, \pm 20$	$-21 \le h \le 3, +5, \pm 20$	$\pm 21, +5, \pm 20$
total no. reflections	6027	3592	5906
independent reflections	1561 ($R_{int} = 0.1808$)	1539 ($R_{int} = 0.1230$)	1529 ($R_{int} = 0.1447$)
reflections with $I > 2\sigma(I)$	720	698	788
data/restraints/parameters	1561/0/80	1539/0/81	1529/0/81
goodness-of-fit on F^2	1.054	1.041	1.073
final R indices [$I > 2\sigma(I)$]	R1 = 0.0366	R1 = 0.0384	R1 = 0.0374
	wR2 = 0.0515	wR2 = 0.0523	wR2 = 0.0659
indices (all data)	R1 = 0.1602	R1 = 0.1674	R1 = 0.1324
	wR2 = 0.0788	wR2 = 0.0800	wR2 = 0.0954
extinction coefficient	0.000059(5)	0.000048(4)	0.00006(1)
largest diff. peak and hole	6.85 and −6.07 e/Å^3	4.91 and −5.92 e/Å^3	5.19 and −4.53 e/Å^3

$CePd_2Sn_2$[10,11] ($CaBe_2Ge_2$ type), Ce_2Pd_2Sn[12,13] (ordered U_3Si_2 type), and $Ce_8Pd_{24}Sn$[14,15] (Cu_3Au superstructure) order antiferromagnetically at Néel temperatures of 7, 0.5, 4.8, and 7.5 K, respectively. The stannides "$Ce_4Pd_7Sn_4$" (structure yet unsolved)[14] and $CePd_{0.5}Sn_2$[14] (defect $CeNiSi_2$ type) show experimental magnetic moments of 2.53 μ_B/Ce, respectively 2.60 μ_B/Ce, compatible with trivalent cerium. Magnetic ordering, however, has not been observed down to 4.2 K.

In the course of our investigations on structure−property relationships of intermetallic cerium compounds[16−19] we have recently synthesized the stannide $CeRhSn_2$[20] which crystallizes with a new structure type. When searching for a possible isotypic compound with palladium as transition metal component, we obtained the stannide $Ce_3Pd_4Sn_6$ and the isotypic compounds $La_3Pd_4Sn_6$ and $Pr_3Pd_4Sn_6$. Herein we report on the synthesis, the structure refinements, and the physical properties of these new stannides.

Experimental Procedures

Synthesis. Starting materials for the synthesis of $La_3Pd_4Sn_6$, $Ce_3Pd_4Sn_6$, and $Pr_3Pd_4Sn_6$ were ingots of lanthanum (Kelpin), of cerium (Johnson Matthey), and of praseodym (Kelpin), palladium powder (200 mesh, Degussa), and a tin bar (Heraeus), all with stated purities better than 99.9%. In a first step the rare earth ingots were cut into small pieces under dried paraffin oil. The latter was washed off with dried (over sodium wire) *n*-hexane and the rare earth pieces were melted into buttons in an arc-melting furnace[21] under an argon atmosphere. This premelting procedure minimizes a shattering of these elements during the strongly exothermic reactions with palladium and tin. The argon was purified before over titanium sponge and molecular sieves. In the second step, the lanthanoid buttons were arc-melted together with cold-pressed pellets (diameter 6 mm) of palladium powder and pieces of the tin bar in the ideal atomic ratio 3:4:6. The buttons were turned over and remelted at least four times to achieve homogeneity. The total weight losses during the arc-melting procedures were all smaller than 0.5 wt %. Finally, fragments of the melted ingots were enclosed in evacuated silica tubes and annealed at 970 K for 3 weeks.

The three stannides are stable in moist air over months. They are dark gray in polycrystalline form while the silvery single crystals exhibit metallic luster. The samples were routinely characterized by EDX analyses of polished ingots using a Leica 420 I scanning electron microscope with LaB_6, CeO_2, PrF_3, palladium, and tin as standards. The compositions were all close to the ideal values. No impurity elements heavier than sodium ($Z = 11$) could be detected. The analyses of the polished ingots in backscattering mode showed only the compositions $La_3Pd_4Sn_6$, $Ce_3Pd_4Sn_6$, and $Pr_3Pd_4Sn_6$.

Structural Characterization. The samples were routinely characterized through their Guinier powder patterns using Cu Kα1 radiation and α quartz ($a = 491.30$ pm, $c = 540.46$ pm) as an internal standard. The patterns could completely be indexed on the basis of primitive orthorhombic cells with the lattice parameters listed in Table 1. To ensure correct indexing, the observed patterns were compared with calculated ones[22] taking the positions of the refined structures.

Small irregularly shaped single crystals of $La_3Pd_4Sn_6$, $Ce_3Pd_4Sn_6$, and $Pr_3Pd_4Sn_6$ could be isolated from the annealed samples by mechanical fragmentation. They were investigated on a Buerger precession camera to establish both symmetry and suitability for intensity data collection. The photographs showed primitive orthorhombic unit cells and the extinction conditions were compatible with space group *Pnma* (no. 62).

(10) Selsane, M.; Lebail, M.; Hamadoui, N.; Kappler, J. P.; Noël, H.; Achard, J. C.; Godart, C. *Physica B* **1990**, *163*, 213.
(11) Lidström, E.; Ghandour, A. M.; Häggström, L.; Andersson, Y. *J. Alloys Compd.* **1996**, *232*, 95.
(12) Gordon, R. A.; Ijiri, Y.; Spencer, C. M.; DiSalvo, F. J. *J. Alloys Compd.* **1995**, *224*, 101.
(13) Chevalier, B.; Fourgeot, F.; Laffargue, D.; Etourneau, J.; Bourée, F.; Roisnel, T. *Physica B* **1997**, *230−232*, 195.
(14) Gordon, R. A.; DiSalvo, F. J. *J. Alloys Compd.* **1996**, *238*, 57.
(15) Gordon, R. A.; DiSalvo, F. J. *Z. Naturforsch. B* **1996**, *51*, 52.
(16) Pöttgen, R.; Borrmann, H.; Felser, C.; Jepsen, O.; Henn, R.; Kremer, R. K.; Simon, A. *J. Alloys Compd.* **1996**, *235*, 170.
(17) Gordon, R. A.; DiSalvo, F. J.; Pöttgen, R.; Brese, N. E. *J. Chem. Soc., Faraday Trans.* **1996**, *92*, 2167.
(18) Jones, C. D. W.; Gordon, R. A.; DiSalvo, F. J.; Pöttgen, R.; Kremer, R. K. *J. Alloys Compd.* **1997**, *260*, 50.
(19) Pöttgen, R.; Hoffmann, R.-D.; Sampathkumaran, E. V.; Das, I.; Mosel, B. D.; Müllmann, R. *J. Solid State Chem.* **1997**, *134*, 326.
(20) Niepmann, D.; Pöttgen, R.; Künnen, B.; Kotzyba, G.; Rosenhahn, C.; Mosel, B. D. *Chem. Mater.* **1999**, *11*, 1597.
(21) Pöttgen, R.; Gulden, Th.; Simon, A. *GIT Labor-Fachzeitschrift* **1999**, *43*, 133.
(22) Yvon, K.; Jeitschko, W.; Parthé, E. *J. Appl. Crystallogr.* **1977**, *10*, 73.

Intensity data were recorded at room temperature by use of a four-circle diffractometer (CAD4) with graphite monochromatized Mo Kα radiation (λ = 71.073 pm) and a scintillation counter with pulse−height discrimination. The scans were taken in the $\omega/2\theta$ mode and empirical absorption corrections were applied on the basis of ψ-scan data.

The structure of the cerium compound was determined first. The starting atomic parameters were deduced from an automatic interpretation of direct methods with SHELXS-97,[23] and the structure was sucessfully refined with anisotropic displacement parameters using SHELXL-97[24] (full-matrix least-squares on F^2). The refined positions of $Ce_3Pd_4Sn_6$ were then taken as starting parameters for the lanthanum and the praseodym compound.

The refinements readily converged to the residuals listed in Table 1 and subsequent difference Fourier syntheses revealed no significant residual peaks. All relevant crystallographic details are listed in Table 1. Atomic coordinates and interatomic distances are given in Tables 2 and 3.

As a check for the correct compositions, the occupancy parameters were varied in a separate series of least-squares cycles along with the displacement parameters. The refined occupancies are listed in Table 2. With the exception of the Pd1 position of $Ce_3Pd_4Sn_6$ and $Pr_3Pd_4Sn_6$ all sites were fully occupied within two standard deviations, and in the final cycles the ideal compositions were assumed. Since the single crystal of $Ce_3Pd_4Sn_6$ was selected from a sample of the starting composition Ce:Pd:Sn 3:3:6 (our first experiments were attempts to synthesize new 1:1:2 stannides), the small defect on one palladium site is comprehensible. The crystals of the lanthanum and the praseodym compound were taken from samples of the intended 3:4:6 compositions. Listings of the anisotropic displacement parameters and the structure factors are available.[25]

Physical Property Investigations. The magnetic susceptibilities of polycrystalline pieces of $La_3Pd_4Sn_6$, $Ce_3Pd_4Sn_6$, and $Pr_3Pd_4Sn_6$ were determined with a SQUID magnetometer (Quantum Design, Inc.) in the temperature range from 2 to 300 K with magnetic flux densities up to 5.5 T. The specific resistivities were measured on small irregularly shaped polycrystalline blocks (typical dimensions 1 × 1 × 2 mm^3) using a four-probe technique. Cooling and heating curves measured between 4.2 and 300 K were identical within the error limits, also for different samples. ^{119}Sn Mössbauer spectroscopic experiments were performed at 300 K with a $Ca^{119m}SnO_3$ source on the same polycrystalline samples as used for the magnetic and electrical measurements. A palladium foil of 0.05 mm thickness was used to reduce the thin K X-rays concurrently emitted by the source.

Table 2. Atomic Coordinates and Isotropic Displacement Parameters for $La_3Pd_4Sn_6$, $Ce_3Pd_4Sn_6$, and $Pr_3Pd_4Sn_6$[a]

atom	occupancy[b]	*x*	*z*	U_{eq}[c]
		$La_3Pd_4Sn_6$		
La1	1.00(3)	0.1411(1)	0.8812(1)	88(4)
La2	0.99(3)	0.3508(1)	0.0172(1)	64(4)
La3	1.01(4)	0.3845(1)	0.7511(1)	108(4)
Pd1	1.00(4)	0.0113(2)	0.1214(2)	131(6)
Pd2	1.01(4)	0.0471(1)	0.4004(2)	86(6)
Pd3	0.99(4)	0.2825(1)	0.2329(2)	82(6)
Pd4	0.99(4)	0.2912(2)	0.5264(2)	108(6)
Sn1	0.99(3)	0.0258(1)	0.5829(2)	87(5)
Sn2	0.98(3)	0.1709(1)	0.1054(1)	78(5)
Sn3	0.99(4)	0.1890(1)	0.6636(2)	89(5)
Sn4	0.99(3)	0.2064(1)	0.3792(2)	77(5)
Sn5	1.00(4)	0.4430(1)	0.2303(2)	105(5)
Sn6	1.01(4)	0.4476(1)	0.5381(2)	97(5)
		$Ce_3Pd_4Sn_6$		
Ce1	1.02(4)	0.1421(1)	0.8811(1)	90(4)
Ce2	0.99(4)	0.3504(1)	0.0175(1)	64(4)
Ce3	1.01(4)	0.3844(1)	0.7519(1)	93(4)
Pd1	0.92(3)	0.0107(2)	0.1215(2)	117(11)
Pd2	0.99(4)	0.0474(2)	0.4002(2)	96(7)
Pd3	0.98(4)	0.2827(2)	0.2333(2)	98(6)
Pd4	1.01(4)	0.2914(2)	0.5263(2)	101(7)
Sn1	1.00(4)	0.0259(1)	0.5815(2)	88(5)
Sn2	1.00(4)	0.1702(2)	0.1062(2)	87(6)
Sn3	1.00(4)	0.1888(2)	0.6631(2)	91(6)
Sn4	0.98(4)	0.2062(2)	0.3795(2)	82(6)
Sn5	0.98(4)	0.4433(2)	0.2307(2)	138(6)
Sn6	0.97(4)	0.4486(2)	0.5386(2)	103(6)
		$Pr_3Pd_4Sn_6$		
Pr1	1.00(4)	0.1426(1)	0.8810(1)	106(4)
Pr2	0.99(4)	0.3498(1)	0.0166(1)	64(4)
Pr3	1.02(4)	0.3847(1)	0.7523(1)	112(4)
Pd1	0.92(4)	0.0095(2)	0.1224(2)	125(10)
Pd2	1.00(4)	0.0475(1)	0.3999(2)	98(5)
Pd3	1.01(4)	0.2823(1)	0.2327(2)	110(5)
Pd4	0.98(4)	0.2922(1)	0.5250(2)	112(6)
Sn1	1.00(4)	0.0262(1)	0.5808(2)	86(5)
Sn2	1.01(4)	0.1697(1)	0.1062(2)	99(5)
Sn3	1.01(4)	0.1893(1)	0.6624(2)	95(5)
Sn4	1.03(4)	0.2061(1)	0.3796(2)	93(5)
Sn5	1.00(4)	0.4428(1)	0.2298(2)	139(5)
Sn6	0.98(4)	0.4495(1)	0.5389(2)	119(5)

[a] All atoms occupy the Wyckoff site 4*c* (*x*1/4*z*) of space group *Pnma*. [b] The occupancy parameters were obtained in separate series of least-squares cycles. In the final cycles the ideal occupancies were assumed with the exception of the Pd1 sites of $Ce_3Pd_4Sn_6$ and $Pr_3Pd_4Sn_6$. [c] U_{eq} (pm^2) is defined as one-third of the trace of the orthogonalized U_{ij} tensor.

Results and Discussion

Magnetic Properties. The temperature dependence of the magnetic susceptibility of $La_3Pd_4Sn_6$ is displayed in Figure 1. The susceptibilities were only weakly dependent on the external field, indicating only very small amounts of ferromagnetic impurities. The 1 and 3 T data were practically identical. The 3 T data are plotted in Figure 1. Down to about 50 K the susceptibilities are very small and nearly independent of temperature. The upturn below 50 K may be attributed to a minor degree of paramagnetic impurities, although our Guinier diagrams showed single phase $La_3Pd_4Sn_6$. The susceptibility at 300 K is 0.7(2) × 10^{-9} m^3/mol, indicating Pauli paramagnetism. This is in agreement with the metallic behavior discussed below.

In Figure 2 we present the temperature dependence of the inverse susceptibilities of $Ce_3Pd_4Sn_6$ and $Pr_3Pd_4Sn_6$. Above 50 K we observe Curie−Weiss behavior with experimental magnetic moments of μ_{exp} = 2.51(2) μ_B/Ce and μ_{exp} = 3.70(5) μ_B/Pr. The experimental moment for $Ce_3Pd_4Sn_6$ compares well with the free ion value of μ_{eff} = 2.54 μ_B for Ce^{3+}. For $Pr_3Pd_4Sn_6$, the experimental moment is slightly higher than the value of 3.58 μ_B for the free Pr^{3+} ion. The paramagnetic Curie temperatures (Weiss constant) of Θ = −27(2) K ($Ce_3Pd_4Sn_6$) and Θ = 3(2) K ($Pr_3Pd_4Sn_6$) were obtained by linear extrapolation of the high-temperature part of the 1/χ vs *T* plot to 1/χ = 0. The strongly negative Weiss constant suggests antiferromagnetic ordering of the cerium compound at very low temperatures.

Below 50 K the inverse susceptibility of $Ce_3Pd_4Sn_6$ significantly deviates from Curie−Weiss behavior, indicating crystal field splitting of the $J = {}^5/_2$ ground state

(23) Sheldrick, G. M. *SHELXS-97, Program for the Solution of Crystal Structures*; University of Göttingen: Göttingen, Germany, 1997.

(24) Sheldrick, G. M. *SHELXL-97, Program for Crystal Structure Refinement*; University of Göttingen: Göttingen, Germany, 1997.

(25) Details may be obtained from: Fachinformationzentrum Karlsruhe, D-76344 Eggenstein-Leopoldshafen (Germany), by quoting the Registry numbers CSD-410987 ($La_3Pd_4Sn_6$), CSD-410988 ($Ce_3Pd_4Sn_6$), and CSD-410986 ($Pr_3Pd_4Sn_6$). E-mail: crysdata@fiz-karlsruhe.de.

Table 3. Interatomic Distances (pm) in the Structures of $La_3Pd_4Sn_6$, $Ce_3Pd_4Sn_6$, and $Pr_3Pd_4Sn_6$[a]

$La_3Pd_4Sn_6$								$Ce_3Pd_4Sn_6$								$Pr_3Pd_4Sn_6$							
La1:	2	Pd4	343.5	Pd4:	1	Sn6	264.3	Ce1:	2	Pd4	340.9	Pd4:	1	Sn6	264.5	Pr1:	2	Pd4	338.1	Pd4:	1	Sn6	264.1
	2	Pd1	345.7		2	Sn2	269.8		2	Sn4	342.8		2	Sn2	268.8		2	Sn4	341.3		1	Sn4	268.0
	2	Sn4	345.7		1	Sn4	270.7		2	Pd1	344.2		1	Sn4	269.6		2	Pd1	342.1		2	Sn2	268.8
	1	Sn3	349.5		1	Sn3	275.0		1	Sn6	347.9		1	Sn3	273.8		1	Sn6	346.4		1	Sn3	274.3
	1	Sn6	349.7		2	La2	333.0		1	Sn3	348.1		2	Ce2	330.9		2	Pd3	348.1		2	Pr2	330.1
	2	Pd3	351.8		2	La1	343.5		2	Pd3	348.5		2	Ce1	340.9		1	Sn3	348.6		2	Pr1	338.1
	1	Sn2	354.0		1	La3	384.8		1	Sn2	353.5		1	Ce3	384.1		1	Sn2	353.0		1	Pr3	385.7
	2	Sn5	359.4	Sn1:	2	Pd2	263.1		2	Sn5	357.7	Sn1:	2	Pd2	261.9		2	Sn5	357.6	Sn1:	2	Pd2	261.5
	2	Sn6	368.7		1	Pd2	287.3		2	Sn6	368.7		1	Pd2	284.5		2	Sn6	369.1		1	Pd2	283.5
	1	La2	412.4		1	Sn3	302.6		1	Ce2	409.0		1	Sn3	301.5		1	Pr2	406.0		1	Sn3	301.0
	1	Pd1	434.5		2	La2	327.5		1	Pd1	434.2		2	Ce2	325.1		1	Pd1	436.4		2	Pr2	324.5
	1	La3	457.9		2	Sn5	330.5		1	Ce3	453.6		2	Sn5	330.5		1	Pr3	451.9		2	Sn5	329.5
	2	La1	462.4		1	La2	334.0		2	Ce1	458.9		1	Ce2	332.3		2	Pr1	457.3		1	Pr2	331.8
	1	La3	479.3		1	La3	352.1		1	Ce3	479.4		1	Ce3	351.5		1	Pr3	478.8		2	Sn1	350.9
La2:	2	Sn1	327.5		2	Sn1	357.9	Ce2:	2	Sn1	325.1		2	Sn1	352.9	Pr2:	2	Sn1	324.5		1	Pr3	351.2
	2	Sn4	330.5	Sn2:	2	Pd4	269.8		2	Sn4	328.2	Sn2:	1	Pd1	268.7		2	Sn4	326.1	Sn2:	2	Pd4	268.8
	2	Sn3	332.0		1	Pd1	270.1		2	Sn3	329.1		2	Pd4	268.8		2	Sn3	328.5		1	Pd1	269.3
	2	Pd4	333.0		1	Pd3	274.0		2	Pd4	330.9		1	Pd3	273.4		2	Pd4	330.1		1	Pd3	272.4
	1	Sn2	333.0		2	Sn6	323.1		1	Sn1	332.3		2	Sn6	321.7		1	Sn1	331.8		2	Sn6	320.9
	1	Sn1	334.0		1	La2	333.0		1	Sn2	332.5		1	Ce2	332.5		1	Sn2	332.1		1	Pr2	332.1
	2	Pd2	341.2		2	La3	337.7		2	Pd2	339.7		2	Ce3	335.3		2	Pd2	338.7		2	Pr3	334.8
	1	Pd2	355.1		2	Sn3	342.8		1	Pd2	354.5		2	Sn3	341.3		1	Pd3	354.4		2	Sn3	340.0
	1	Pd3	356.0		1	La1	354.0		1	Pd3	354.5		1	Ce1	353.5		1	Pd2	355.4		1	Pr1	353.0
	1	Sn5	367.4	Sn3:	2	Pd3	259.8		1	Sn5	366.5	Sn3:	2	Pd3	258.6		1	Sn5	366.0	Sn3:	2	Pd3	257.8
	1	La1	412.4		1	Pd4	275.0		1	Ce1	409.0		1	Pd4	273.8		1	Pr1	406.0		1	Pd4	274.3
	1	La3	419.7		1	Sn1	302.6		1	Ce3	417.2		1	Sn1	301.5		1	Pr3	414.9		1	Sn1	301.0
	2	La2	462.4		2	La2	332.0		2	Ce2	458.9		2	Ce2	329.1		2	Pr2	457.3		2	Pr2	328.5
La3:	2	Sn2	337.7		2	Sn5	337.3	Ce3:	2	Sn2	335.3		2	Sn5	335.9	Pr3:	2	Sn2	334.8		2	Sn5	334.9
	2	Sn4	342.1		2	Sn2	342.8		2	Sn4	339.4		2	Sn2	341.3		2	Sn4	338.3		2	Sn2	340.0
	2	Pd2	348.1		1	La1	349.5		2	Pd2	344.9		1	Ce1	348.1		2	Pd2	343.2		1	Pr1	348.6
	1	Sn6	349.5		1	La3	356.8		1	Sn6	349.0		1	Ce3	356.2		1	Sn6	349.0		1	Pr3	355.6
	1	Sn1	352.1	Sn4:	1	Pd3	262.2		1	Sn1	351.5	Sn4:	1	Pd3	261.3		1	Sn1	351.2	Sn4:	1	Pd3	261.5
	2	Pd1	354.0		1	Pd2	270.6		2	Pd1	353.3		1	Pd2	268.4		2	Pd1	352.8		1	Pd2	267.2
	1	Sn3	356.8		1	Pd4	270.7		1	Sn3	356.2		1	Pd4	269.6		1	Sn3	355.6		1	Pd4	268.0
	2	Pd3	365.4		2	La2	330.5		2	Pd3	363.5		2	Ce2	328.2		2	Pd3	362.3		2	Pr2	326.1
	2	Sn5	372.6		2	La3	342.1		2	Sn5	370.2		2	Ce3	339.4		2	Sn5	369.5		2	Pr3	338.3
	1	Pd4	384.8		2	La1	345.7		1	Pd4	384.1		2	Ce1	342.8		1	Pd4	385.7		2	Pr1	341.3
	1	La2	419.7	Sn5:	1	Pd1	258.8		1	Ce2	417.2	Sn5:	1	Pd1	256.5		1	Pr2	414.9	Sn5:	1	Pd1	255.4
	1	La1	457.9		1	Pd2	269.3		1	Ce1	453.6		1	Pd2	268.3		1	Pr1	451.9		1	Pd2	267.1
	2	La3	462.4		1	Pd3	270.4		2	Ce3	458.9		1	Pd3	269.5		2	Pr3	457.3		1	Pd3	268.7
	1	La1	479.3		2	Sn1	330.5		1	Ce1	479.4		2	Sn1	330.5		1	Pr1	478.8		2	Sn1	329.5
Pd1:	1	Sn5	258.8		2	Sn3	337.3	Pd1:	1	Sn5	256.5		2	Sn3	335.9	Pd1:	1	Sn5	255.4		2	Sn3	334.8
	1	Sn2	270.1		2	La1	359.4		1	Sn2	268.7		2	Ce1	357.7		1	Sn2	269.3		2	Pr1	357.6
	1	Sn6	271.4		1	La2	367.4		1	Sn6	270.0		1	Ce2	366.5		1	Sn6	270.1		1	Pr2	366.0
	2	Sn6	274.2		2	La3	372.6		2	Sn6	271.9		2	Ce3	370.2		2	Sn6	271.8		2	Pr3	369.5
	2	La1	345.7	Sn6:	1	Pd4	264.3		2	Ce1	344.2	Sn6:	1	Pd4	264.5		2	Pr1	342.1	Sn6:	1	Pd4	264.1
	2	La3	354.0		1	Pd1	271.4		2	Ce3	353.3		1	Pd1	270.0		2	Pr3	352.8		1	Pd1	270.1
Pd2:	2	Sn1	263.1		2	Pd1	274.2	Pd2:	2	Sn1	261.9		2	Pd1	271.9	Pd2:	2	Sn1	261.5		2	Pd1	271.8
	1	Sn5	269.3		2	Sn6	314.3		1	Sn5	268.3		2	Sn6	311.2		1	Sn5	267.1		2	Sn6	309.1
	1	Sn4	270.6		2	Sn2	323.1		1	Sn4	268.4		2	Sn2	321.7		1	Sn4	267.2		2	Sn2	320.9
	1	Sn1	287.3		1	La3	349.5		1	Sn1	284.5		1	Ce1	348.0		1	Sn1	283.5		1	Pr1	346.4
	2	La2	341.2		1	La1	349.7		2	Ce2	339.7		1	Ce3	349.0		2	Pr2	338.7		1	Pr3	349.0
	2	La3	348.1		2	La1	368.7		2	Ce3	344.9		2	Ce1	368.7		2	Pr3	343.2		2	Pr1	369.1
	1	La2	355.1						1	Ce2	354.5						1	Pr2	355.4				
Pd3:	2	Sn3	259.8					Pd3:	2	Sn3	258.6					Pd3:	2	Sn3	257.9				
	1	Sn4	262.2						1	Sn4	261.3						1	Sn4	261.5				
	1	Sn5	270.4						1	Sn5	269.5						1	Sn5	268.7				
	1	Sn2	274.0						1	Sn2	273.4						1	Sn2	272.4				
	2	La1	351.8						2	Ce1	348.5						2	Pr1	348.1				
	1	La2	356.0						1	Ce2	354.5						1	Pr2	354.4				
	2	La3	365.4						2	Ce3	363.5						2	Pr3	362.3				

[a] All distances of the first coordination spheres are listed. Standard deviations are all equal or less than 0.4 pm.

of the Ce^{3+} ions, but also the beginning of short-range magnetic fluctuations. Such crystal field effects may also account for the broad shoulder in the electric resistivity at high temperature (see Figure 4 below).

The magnetic behavior of $Ce_3Pd_4Sn_6$ and $Pr_3Pd_4Sn_6$ at low temperature and low external fields (0.1 T) is presented in the inserts of Figure 2. Down to 2 K no indication for magnetic ordering could be observed.

The magnetization data are plotted in Figure 3. At 50 K the magnetization isotherms of $Ce_3Pd_4Sn_6$ and $Pr_3Pd_4Sn_6$ are almost linear as expected for a paramagnetic compound. The isotherms then show some curvature at 2 K, however, with different saturation magnetization values at 5.5 T: 0.78(1) μ_B/Ce and 0.39(1) μ_B/Pr, significantly smaller than the theoretical saturation magnetizations for Ce^{3+} and Pr^{3+} of 2.14 μ_B/Ce and 3.20 μ_B/Pr. $Pr_3Pd_4Sn_6$ most likely remains paramagnetic down to very low temperatures as is also manifested by the very small paramagnetic Curie temperature of 3(2) K. $Ce_3Pd_4Sn_6$ shows a stronger increase of the

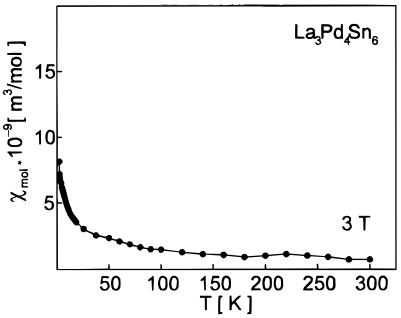

Figure 1. Temperature dependence of the magnetic susceptibility of $La_3Pd_4Sn_6$, measured at a flux density of 3 T.

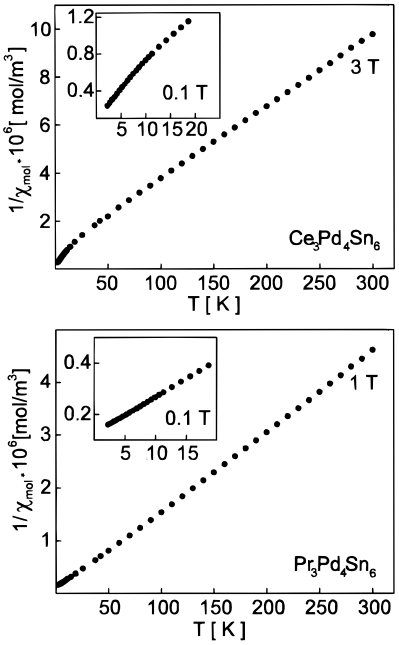

Figure 2. Temperature dependence of the inverse magnetic susceptibilities of $Ce_3Pd_4Sn_6$ and $Pr_3Pd_4Sn_6$ measured at 1 and 3 T. The behavior at low temperature and low flux density (0.1 T) is shown in the inserts.

magnetic moment at 2 K. This may be attributed to a partial antiparallel to parallel spin alignment. The reduced value of the saturation moment is most likely due to crystal field splitting effects on the $J = 5/2$ ground state of the Ce^{3+} ion. Similar moments in the range of 1 μ_B/Ce atom have also been observed for similar ternary cerium intermetallics, i.e., 0.75(2) μ_B for $CeRhSn_2$,[20] 1.09(5) μ_B for CeAuGe,[26] and even 0.64 μ_B/Ce for CePtSb.[27] Neutron diffraction experiments may be helpful in future to further elucidate the nature of magnetic ordering in this cerium stannide.

Electrical Properties. The temperature dependence of the specific resistivities of $La_3Pd_4Sn_6$, $Ce_3Pd_4Sn_6$, and $Pr_3Pd_4Sn_6$ is displayed in Figure 4. The specific resistivity of all three stannides decreases with decreasing temperature as expected for a metal. The room-temperature values are 80 ± 20 $\mu\Omega$ cm ($La_3Pd_4Sn_6$), 65 ± 20 $\mu\Omega$ cm ($Ce_3Pd_4Sn_6$), and 110 ± 20 $\mu\Omega$ cm ($Pr_3Pd_4Sn_6$). The relatively large error limit accounts for the different values obtained for several irregularly shaped samples. At 4.2 K, the specific resistivity has dropped to 16 ± 5 $\mu\Omega$ cm ($La_3Pd_4Sn_6$), 25 ± 5 $\mu\Omega$ cm ($Ce_3Pd_4Sn_6$), and 14 ± 5 $\mu\Omega$ cm ($Pr_3Pd_4Sn_6$), resulting in resistivity ratios ρ(4.2 K)/ρ(300 K) of about 0.20 ($La_3Pd_4Sn_6$), 0.39 ($Ce_3Pd_4Sn_6$), and 0.13 ($Pr_3Pd_4Sn_6$). Features worthy of note in the plot of $Ce_3Pd_4Sn_6$ are the broad region of negative curvature between 40 and 300 K and a broad minimum near 16 K. The latter was also observed for $CeRhSn_2$,[20] CePdSn[9,28] and $Ce_3Pd_6Sb_5$[29] and may be due to the presence of some Kondo-like interactions, however, an explanation of increased scattering due to increased magnetic fluctuations at low temperature is also possible.

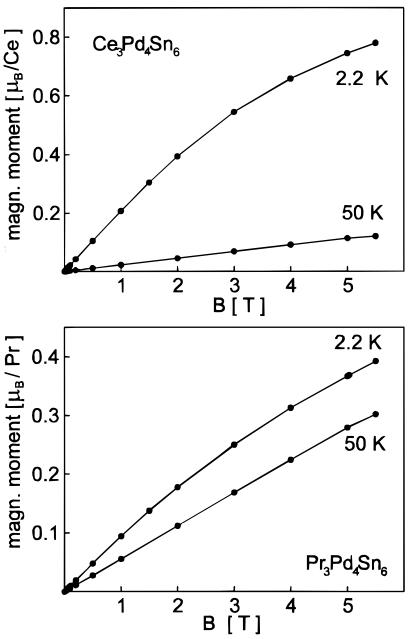

Figure 3. Field dependence of the magnetic moments of $Ce_3Pd_4Sn_6$ and $Pr_3Pd_4Sn_6$ at 2.2 and 50 K.

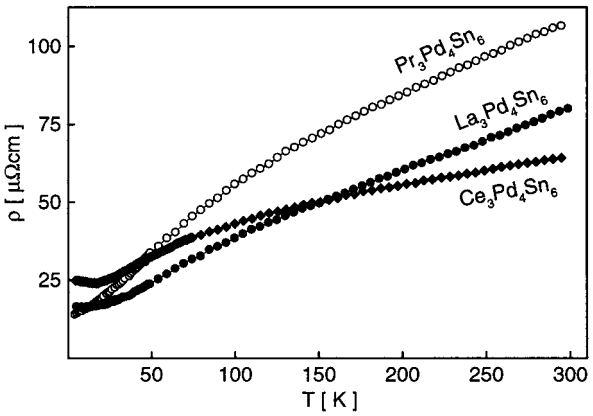

Figure 4. Temperature dependence of the specific resistivities of $La_3Pd_4Sn_6$, $Ce_3Pd_4Sn_6$, and $Pr_3Pd_4Sn_6$.

^{119}Sn Mössbauer Spectroscopy. The room temperature ^{119}Sn Mössbauer spectra of $La_3Pd_4Sn_6$, $Ce_3Pd_4Sn_6$, and $Pr_3Pd_4Sn_6$ are presented in Figure 5 together with theoretical transmission integral fits. The fitting parameters are listed in Table 4. The spectra are more or less equal. We therefore discuss only the lanthanum compound and refer to Table 4 for the other data. The

(26) Pöttgen, R.; Borrmann, H.; Kremer, R. K. *J. Magn. Magn. Mater.* **1996**, *152*, 196.
(27) Rainford, B. D.; Adroja, D. T. *Physica B* **1994**, *194/196*, 365.
(28) Malik, S. K.; Adroja, D. T.; Dhar, S. K.; Vijayaraghavan, R.; Padalia, B. D. *Phys. Rev. B* **1989**, *40*, 2414.
(29) Gordon, R. A.; DiSalvo, F. J.; Pöttgen, R. *J. Alloys Compd.* **1995**, *228*, 16.

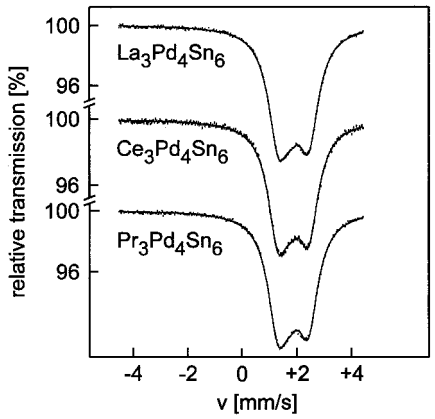

Figure 5. Experimental and simulated ^{119}Sn Mössbauer spectra of $La_3Pd_4Sn_6$, $Ce_3Pd_4Sn_6$, and $Pr_3Pd_4Sn_6$ at 300 K relative to $Ca^{119}SnO_3$.

Table 4. Fitting Parameters of ^{119}Sn Mössbauer Measurements (300 K) of $La_3Pd_4Sn_6$, $Ce_3Pd_4Sn_6$, and $Pr_3Pd_4Sn_6$[a]

compound	Γ_1 (mm/s)	δ_1 (mm/s)	ΔE_{Q1} (mm/s)	Γ_2 (mm/s)	δ_2 (mm/s)	ratio[b]
$La_3Pd_4Sn_6$	0.87(2)	1.94(2)	1.11(2)	0.88(2)	1.88(2)	5.2:1
$Ce_3Pd_4Sn_6$	0.85(2)	1.93(2)	1.13(2)	0.97(2)	1.87(2)	4.1:1
$Pr_3Pd_4Sn_6$	0.85(2)	1.92(2)	1.12(2)	0.98(2)	1.85(2)	4.8:1

[a] Abbreviations: Γ, experimental line width; δ, isomer shift; ΔE_Q, electric field gradient. The indices 1 and 2 refer to the doublet and singlet signals, respectively. [b] Ratio of the areas of both signals (doublet:singlet).

spectrum shows a superposition of two different signals: a singlet at $\delta_2 = 1.88(2)$ mm/s with a line width of $\Gamma_2 = 0.88(2)$ mm/s and a second signal at $\delta_1 = 1.94(2)$ mm/s with a line width of $\Gamma_1 = 0.87(2)$ mm/s, subject to quadrupole splitting of $\Delta E_{Q1} = 1.11(2)$ mm/s. The integrated peak areas (doublet:singlet) are about 5.2:1. While only the Sn4 atoms have no tin neighbors, the Sn1, Sn2, Sn3, Sn5, and Sn6 atoms have at least one short Sn−Sn contact. From a crystal chemical point of view the tin types have a ratio of 5:1 which is in excellent agreement with the Mössbauer spectra. We thus observed the singlet for the Sn4 site and the doublet for the remaining tin atoms. Since the coordinations of the Sn1, Sn2, Sn3, Sn5, and Sn6 atoms are very similar, the respective Mössbauer signals are most likely indistinguishable. Thus, the doublet is a superimposed signal of five very similar doublets. Such a composed ^{119}Sn Mössbauer spectrum was observed recently also for the stannide YbAgSn[30] which contains a Sn_2 pair and an *isolated* tin atom.

Crystal Chemistry and Chemical Bonding. The ternary stannides $La_3Pd_4Sn_6$, $Ce_3Pd_4Sn_6$, and $Pr_3Pd_4Sn_6$ crystallize with a new orthorhombic structure type which we have first determined for the cerium compound. We therefore call this a $Ce_3Pd_4Sn_6$ type structure. In Figure 6 we present a projection of the $Ce_3Pd_4Sn_6$ structure onto the *xz* plane. When we quote interatomic distances in the following discussion, they refer to the cerium compound.

Three crystallographically different cerium positions with high coordination numbers (CN) occur in the

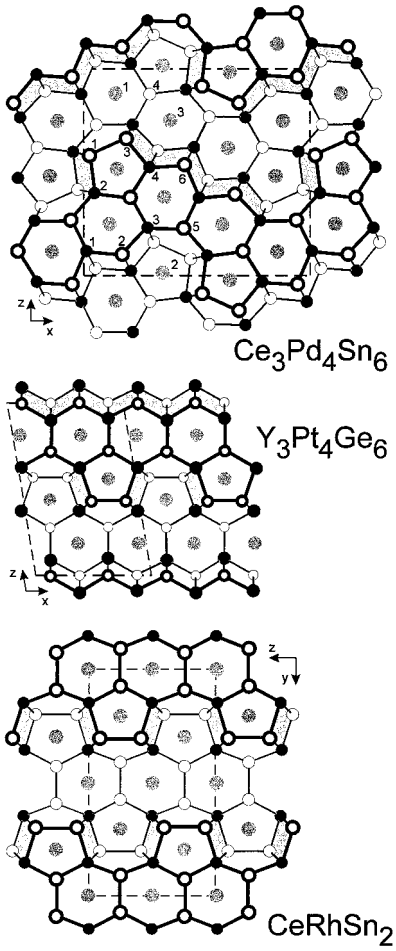

Figure 6. Projections of the crystal structures of $Ce_3Pd_4Sn_6$, $Y_3Pt_4Ge_6$, and $CeRhSn_2$ onto the *xz* and *yz* planes, respectively. The three-dimensional $[Pd_4Sn_6]$, $[Pt_4Ge_6]$, and $[RhSn_2]$ polyanions are outlined. Some Pd_2Sn_2, Pt_2Ge_2, and Rh_2Sn_2 parallelograms are shaded to show the characteristic connectivities of these basic structural units. The different sites in the structure of $Ce_3Pd_4Sn_6$ are given by arabic numbers. The cerium (yttrium), transition metal, and tin (germanium) atoms are drawn as gray, black, and open circles, respectively.

structure of $Ce_3Pd_4Sn_6$: 5Ce + 7Pd + 9Sn for Ce1, 4Ce + 6Pd + 9Sn for Ce2, and 5Ce + 7Pd + 9Sn for Ce3. These high coordination numbers are typical for such intermetallic compounds. The closest Ce−Ce distances range from 409 to 479 pm, much longer than in fcc cerium[31] where each cerium atom has 12 cerium neighbors at 365 pm. Although the Ce−Ce distances in $Ce_3Pd_4Sn_6$ are quite long and these contacts are most likely not bonding, the respective cerium atoms complete the coordination shells as frequently observed for such compounds.[20,32,33]

The Ce−Pd distances range from 325 to 384 pm, significantly longer than the sum of the metallic radii[34] of 320 pm for CN 12, indicating only negligible Ce−Pd interactions. Also in the structure of $Ce_3Pd_6Sb_5$[29] such long Ce−Pd distances (327−367 pm) occur. The Ce−Sn

(30) Pöttgen, R.; Arpe, P. E.; Felser, C.; Kussmann, D.; Müllmann, R.; Mosel, B. D.; Künnen, B.; Kotzyba, G. *J. Solid State Chem.* **1999**, *145*, 668.

(31) Donohue, J. *The Structures of the Elements*; Wiley: New York, 1974.

(32) Hoffmann, R.-D.; Pöttgen, R.; Rosenhahn, C.; Mosel, B. D.; Künnen, B.; Kotzyba, G. *J. Solid State Chem.* **1999**, *145*, 283.

(33) Hoffmann, R.-D.; Pöttgen, R. *Z. Anorg. Allg. Chem.* **1999**, *625*, 994.

(34) Teatum, E.; Gschneidner, K., Jr.; Waber, J. Report LA-2345, U.S. Department of Commerce: Washington, DC, 1960.

distances range from 325 to 370 pm with an average value of 346 pm, in perfect agreement with the sum of the metallic radii[34] for cerium and tin of 345 pm. Also in $CeRhSn_2$,[20] an average Ce−Sn distance of 343 pm has been observed. The shortest Ce−Sn distances occur for the Ce2 site. Here, the six nearest tin neighbors are at Ce−Sn distances from 325 to 329 pm. These Ce−Sn contacts may be considered as weakly bonding, similar to $CeRhSn_2$[20] and $CeRu_4Sn_6$.[19]

The most striking feature of the $Ce_3Pd_4Sn_6$ structure are remarkably short Pd−Sn distances. Each palladium atom has a distorted, square-pyramidal coordination of tin neighbors at Pd−Sn distances ranging from 257 to 285 pm with an average value of 268 pm, in perfect agreement with the sum of Pauling's single bond radii of 268 pm.[35] We therefore assume strong palladium−tin bonding in the structure of $Ce_3Pd_4Sn_6$. This compares well with a recent extended Hückel calculation for $CaPdSn_2$[36] with $MgCuAl_2$ type structure, where the strongest bonding interactions were found for the Pd−Sn contacts followed by Sn−Sn.

Six crystallographically different tin sites occur in the structure of $Ce_3Pd_4Sn_6$ with Sn−Sn distances ranging from 302 to 353 pm. The Sn4 position is an exception. This tin atom has only palladium and cerium neighbors. The shorter Sn1−Sn3 (302 pm), Sn6−Sn6 (311 pm), and Sn2−Sn6 (322 pm) contacts may be considered as at least weakly bonding. These Sn−Sn distances compare well with those in β-tin[31] (4×302 pm; 2×318 pm).

In view of the strongly bonding Pd−Sn and the at least weakly bonding Sn−Sn interactions, also the structure of $Ce_3Pd_4Sn_6$ can best be described by a three-dimensional [Pd_4Sn_6] polyanion in which the cerium atoms fill distorted pentagonal and hexagonal channels as outlined in Figure 6. The basic structural motif of the polyanion are the four $PdSn_5$ units which are condensed with each other via common tin atoms and via Sn−Sn bonds. Considering the trivalent character of the cerium atoms (see magnetic data), the formula of $Ce_3Pd_4Sn_6$ can to a first approximation be written as $[3Ce^{3+}]^{9+}[Pd_4Sn_6]^{9-}$, where the superscripts are formal charges.

The structure of $Ce_3Pd_4Sn_6$ has large similarities with the structures of $CeRhSn_2$[20] and $Y_3Pt_4Ge_6$.[37] Projections of these structures with an emphasis on the [$RhSn_2$] and [Pt_4Ge_6] polyanions are presented in Figure 6. All of these polyanions are composed of edge- and corner-sharing Pd_2Sn_2, Rh_2Sn_2, and Pt_2Ge_2 parallelograms. Such parallelograms also occur in the structures of SrPtIn[33] (TiNiSi type), $CaAuIn_2$[38] ($MgCuAl_2$ type), $Sr_2Au_3In_4$[32] ($Hf_2Co_4P_3$ type), and $Ca_2Au_3In_4$[33] (YCo_5P_3 type), however, with different connectivities. At first sight these structures look quite different; however, a closer look at the respective polyanions shows that they have all T_2X_2 parallelograms as common structural motifs, leading to a rich crystal chemistry.

Acknowledgment. We are indebted to Professor Dr. W. Jeitschko and to Professor Dr. H. Eckert for their interest and steady support of this work. We also thank K. Wagner for the EDX analyses, Dipl.-Ing. U. Ch. Rodewald for the data collections, and Dr. W. Gerhartz (Degussa AG) for a generous gift of palladium powder. Financial support by the Bennigsen-Foerder-Programm of the Ministerium für Wissenschaft und Forschung des Landes Nordrhein-Westfalen, by the Deutsche Forschungsgemeinschaft and by the Fonds der Chemischen Industrie is gratefully acknowledged.

CM991142Z

(35) Pauling, L. *The Nature of the Chemical Bond and the Structures of Molecules and Solids*; Cornell University Press: Ithaca, NY, 1960.

(36) Hoffmann, R.-D.; Kussmann, D.; Rodewald, U. Ch.; Pöttgen, R.; Rosenhahn, C.; Mosel, B. D. *Z. Naturforsch. B* **1999**, *54*, 709.

(37) Venturini, G.; Malaman, B. *J. Less-Common Met.* **1990**, *167*, 45.

(38) Hoffmann, R.-D.; Pöttgen, R.; Landrum, G. A.; Dronskowski, R.; Künnen, B.; Kotzyba, G. *Z. Anorg. Allg. Chem.* **1999**, *625*, 789.